Volume 97, February 2012 • ISSN 0927-0248

Solar Energy Materials and Solar Cells

An international journal devoted to photovoltaic, photothermal and photochemical solar energy conversion

Special Issue:
Dedicated to the Global Organic Photovoltaics (GOPV) conference in Hangzhou, China

Guest Editor: Frederik C. Krebs

GOPV
China | Denmark

Available online at www.sciencedirect.com
SciVerse ScienceDirect

Solar Energy Materials & Solar Cells
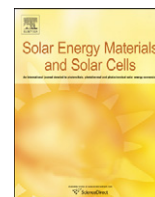
Interlayer adhesion in roll-to-roll processed flexible inverted polymer solar cells

Stephanie R. Dupont [a], Mark Oliver [a], Frederik C. Krebs [b], Reinhold H. Dauskardt [a,*]

[a] Department Materials Science and Engineering, Stanford University, Stanford, CA 94305-2205, USA
[b] Risø National Laboratory for Sustainable Energy, Technical University of Denmark, Frederiksborgvej 399, DK-4000 Roskilde, Denmark

ARTICLE INFO

ABSTRACT

The interlayer adhesion of roll-to-roll processed flexible inverted P3HT:PCBM bulk heterojunction (BHJ) polymer solar cells is reported. Poor adhesion between adjacent layers may result in loss of device performance from delamination driven by the thermomechanical stresses in the device. We demonstrate how a thin-film adhesion technique can be applied to flexible organic solar cells to obtain quantitative adhesion values. For the P3HT:PCBM-based BHJ polymer solar cells, the interface of the BHJ with the conductive polymer layer PEDOT:PSS was found to be the weakest. The adhesion fracture energy varied from 1.6 J/m^2 to 0.1 J/m^2 depending on the composition of the P3HT:PCBM layer. Post-deposition annealing time and temperature were shown to increase the adhesion at this interface. Additionally the PEDOT:PSS cells are compared with V$_2$O$_5$ cells whereby adhesive failure marked by high fracture energies was observed.

© 2011 Elsevier B.V. All rights reserved.

1. Introduction

Roll-to-roll (R2R) processed polymer solar cells are promising due to their low cost, light weight, compatibility with flexible substrates, high throughput processing and large area solar cell production [1–6], although concerns exist regarding their reliability. Many failure modes relevant to polymer solar cells have been identified while there is a general agreement that the majority of failure modes remain uncharted. Until now degradation due to chemical reaction with atmospheric components (oxidation and corrosion) has been studied for laboratory devices on rigid substrates. The general polymer solar cell comprise a multilayer structure where mechanical stability is not automatically granted due to the different mechanical properties for each of the layers and their individual response to the processing conditions (temperature, humidity, solvent vapor, strain, etc). Since most research efforts have focused on achieving higher power conversion efficiencies (PCE) for small area devices on rigid and mechanically stable substrates, little is known about the thermomechanical reliability of polymer solar cells. For example, damage processes such as adhesive and cohesive fracture may result from the thin-film stresses present in the organic solar cells [7]. Thin-film stresses can develop during device processing and operation. During processing the evaporation of solvents may give rise to different shrinkage strains and associated stresses [8]. Thermal strain and associated stresses develop during thermal cycles due to the thermal expansion mismatch of the different layers. Other stresses may result from specific film growth processes such as the coalescence of islands of material as the film is deposited. Finally, bending of the flexible polymer solar cells may cause additional mechanical stresses. It is the combination of these film stresses together with other possible mechanical handling and operation stresses that provide the mechanical driving force for the delamination of weak interfaces or cohesion cracking of weak layers. This leads to a loss of mechanical integrity and device performance. Therefore a fundamental understanding of the interlayer adhesion and strategies for improving the adhesion fracture energy must be developed.

We demonstrate how a thin-film adhesion technique can be applied to flexible R2R processed inverted polymer solar cells on polyethyleneterphthalate (PET) substrates. The adhesion energy required to separate adjacent layers can be precisely measured independent of the solar cell film mechanical properties, thickness and stresses, which greatly simplifies the measurement technique [9]. This provides for quantitative analysis of the impact of various processing and structural variables on adhesion and a means for understanding the mechanisms of delamination. Additionally this enables a compositional analysis of the interfaces of the internal layers.

In this work we report on the adhesion between the photoactive region Poly(3-hexylthiophene):Phenyl-C61-butyric acid methyl ester (P3HT:PCBM) BHJ and hole transport layer (HTL)
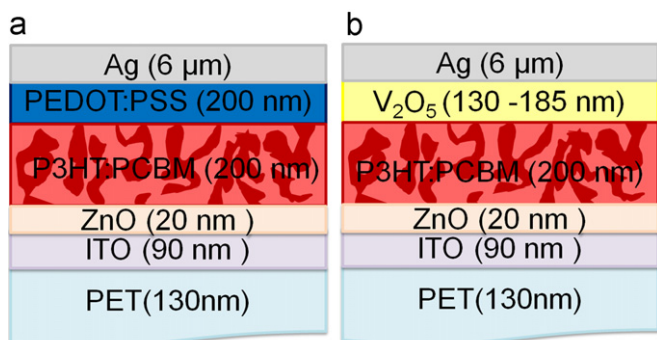
Fig. 1. Device structure of P3HT:PCBM solar cells with either PEDOT:PSS (a) or V_2O_5 (b) as hole transport layer.

Poly(3.4-ethylenedioxythiophene): Poly(styrenesulfonate) (PEDOT:PSS). This interface was found to be the weakest in the R2R inverted polymer solar cells. The adhesion fracture energy varied from 1.6 J/m² to 0.1 J/m² depending on the composition of the P3HT:PCBM layer. Post-deposition annealing was applied to increase the adhesion at this interface. It is shown that the adhesive fracture energies increased with annealing time and temperature. Additionally, delamination in PEDOT-free R2R inverted flexible polymer solar cells has been studied, whereby the conductive polymer PEDOT:PSS has been replaced by a metal oxide HTL, vanadiumoxide (V_2O_5).

2. Experimental

2.1. Solar cell processing

The processing of the R2R inverted polymer solar cells, shown in Fig. 1 has been described elsewhere [10–13]. Briefly, the polymer solar cells were processed using a roll-to-roll automated set-up. A screen printer was used for the ITO and silver electrodes and a slot die coater for the ZnO, BHJ and HTL's. The polymer solar cells were processed on flexible PET substrates covered with transparent ITO electrodes. A thin zinc oxide layer was initially deposited to form an electron selective contact. Then, the photoactive BHJ of an electron donor P3HT (Sepiolid P200 BASF) and electron acceptor PCBM (99%, Solenne B.V.) was deposited. The fraction of PCBM in P3HT:PCBM BHJ was varied between 0 wt% and 100 wt% using a differentially pumped slot die coater. A thin-film of PEDOT:PSS (Agfa 5010) diluted in isopropyl alcohol was slot-die coated on top to serve as the HTL. Additionally cells, whereby the conducting PEDOT:PSS polymer layer was replaced by a hydrated vanadiumoxide layer ($V_2O_5 \cdot (H_2O)_n$), were prepared from a dilution of vanadyl-triisopropoxide (Sigma Aldrich) in isopropanol. The thickness of the V_2O_5 layer was varied between 130 nm and 185 nm, while keeping the composition of P3HT:PCBM at a constant 10:9 ratio. A 6 μm thick silver paste (UV curing Toyo Ink) layer was used as back electrode for both cell structures. Finally, the polymer solar cells were encapsulated using a barrier material (Amcor) and an adhesive (467 MPF, 3M).

2.2. Thin-film adhesion/cohesion testing

The adhesion or cohesion fracture energy is the energy needed to cause delamination at the interface between layers or failure within a layer, respectively. In the case of interface adhesion, delamination occurs if the driving force for debonding, quantified in terms of the applied strain energy release rate, G is larger than a critical value, G_c, the adhesion fracture energy. The fracture energy is determined by two different energy absorbing
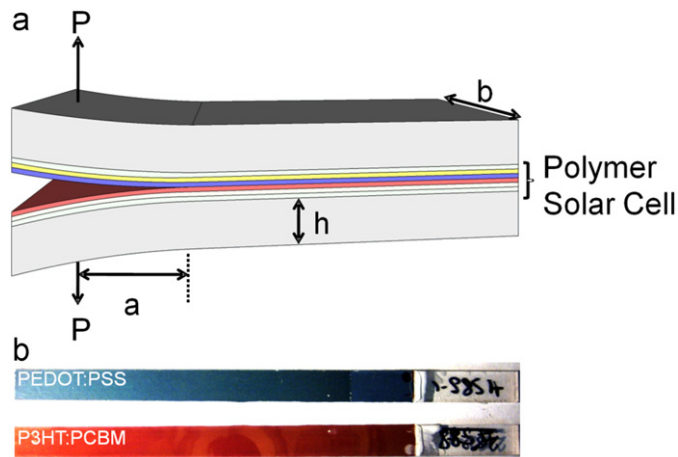

Fig. 2. (a) Illustration of the double cantilever beam (DCB) test specimen. The polymer solar cell is sandwiched between two rectangular elastically stiff beams. (b) Illustration of the debonded surfaces clearly showing adhesive failure between the blue PEDOT:PSS layer (top) and red brown P3HT:PCBM layer (bottom). (For interpretation of the references to color in this figure legend, the reader is referred to the web version of this article).

processes: one involves the near-tip work of fracture including processes such as breaking chemical bonds across the interface and creating new surfaces and the other includes energy dissipation in a zone surrounding the crack [9]. G_c is typically strongly dependent on the material, mechanical and processing properties.

To measure the fracture energy, G_c (J/m^2) the flexible solar cells were epoxy bonded in between two elastic beams to form a double cantilever beam (DCB), as illustrated in Fig. 2. The DCB test geometry is a well-established method for measuring the fracture energy in thin-film structures and interfaces [9,14–16]. Silicon, polycarbonate and aluminum were used as beam materials. The specimens were mounted into the adhesion testing system (Delaminator DTS, Menlo Park, CA). Subsequently the DCB specimens were loaded in a mode I tension from which a load versus displacement curve was recorded. Finally, the fracture energy, G_c can be expressed in terms of the critical load at which crack growth occurs, P_c, the corresponding crack length a, the plain strain elastic modulus, E' and the specimen dimensions width, b and half- thickness, h. The fracture energy was calculated from Eq. 1[17].

$$G_c = \frac{12P_c^2 a^2}{B^2 E' h^3}\left(1 + 0.64\frac{h}{a}\right)^2$$

All testing were carried out in laboratory air environment at ~25 °C and ~45% relative humidity. Following mechanical testing, x-ray photo spectroscopy (XPS, PHI 5000 Versaprobe) was used to determine the location of the fracture path in the polymer solar cell.

3. Results and discussion

3.1. Composition ratio P3HT:PCBM

The fracture energy, G_c measured versus the weight fraction of PCBM in the P3HT:PCBM layer is shown in Fig. 3. G_c reaches values of 1.6 J/m² for a nearly pure P3HT layer (3 wt% PCBM), decreases non-linearly with higher fraction of PCBM in the BHJ and is only 0.1 J/m² for a nearly pure PCBM layer (98 wt% PCBM). The PCE of the PEDOT:PSS cells varied from 0.006% for a 100% P3HT going through a maximum of 2.2% for a 1:1 ratio of P3HT:PCBM layer and decreasing to 0.05% for a 100% PCBM layer

as previously reported [10]. Adhesive failure at the interface of BHJ P3HT:PCBM with conductive polymer layer PEDOT:PSS was observed by XPS for all compositions of P3HT:PCBM, except for the nearly pure PCBM layers mixed adhesive failure was observed. The adhesive fracture path was also visually apparent. The surface of the delaminated specimen with a blue colored PEDOT:PSS surface at one side and the brownish P3HT:PCBM surface at the other side is shown in Fig. 2b.

The hydrophobic P3HT:PCBM and negatively charged hydrophilic PEDOT:PSS form the weakest interface in the inverted flexible polymer solar cells. The BHJ layers with higher concentrations of P3HT form a stronger interface with PEDOT:PSS than the PCBM rich BHJ even though P3HT is slightly more hydrophobic [18]. This can be attributed to the secondary Van Der Waals forces that develop between long chains of P3HT with PEDOT:PSS. In contrast PCBM is a very stable small molecule, which is less likely to form strong secondary bonds. Consequently if more PCBM is added to the

BHJ the interface with PEDOT:PSS will be weaker explaining the observed decrease in fracture energy.

The adhesion energy reported at the BHJ P3HT:PCBM and conductive polymer layer PEDOT:PSS interface is low in comparison with adhesion and cohesion G_c values for common materials used in microelectronic devices [19]. Low adhesion in these device technologies has been associated with low yield during device processing and poor long term reliability. Therefore different strategies to improve the adhesion between the HTL and active layer in inverted polymer solar cells were studied and quantified. The poor wetting of PEDOT:PSS on P3HT:PCBM has already been reported as a problem during the processing of inverted polymer solar cell and therefore several additional processing steps have been used in the past including chemical, thermal, mechanical and plasma treatments [20–22]. However to the best of our knowledge no quantitative measurement of the change in adhesion has been provided so far.
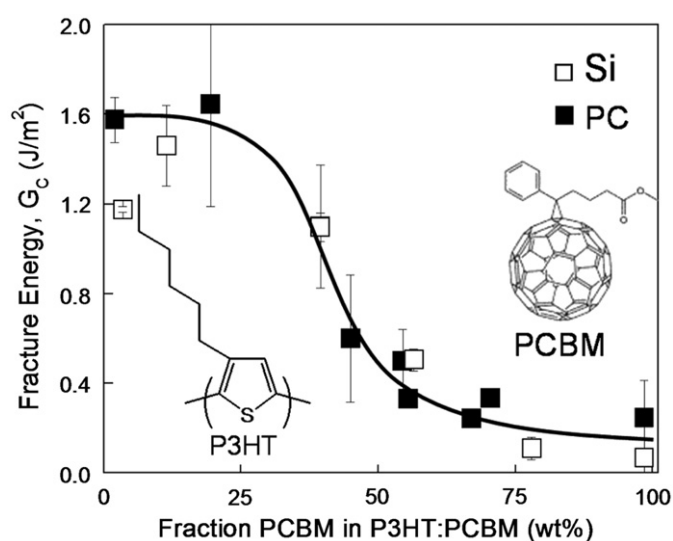
3.2. Post deposition annealing

The fracture energy, G_c as a function of annealing time for the post deposition annealed polymer solar cells is shown in Fig. 4. In Fig. 4a polymer solar cells with different concentrations of PCBM annealed at 130 °C are compared. In Fig.4b G_c as a function of annealing time for 1:1 P3HT:PCBM polymer solar cells annealed at 110 °C and 130 °C. An increase of fracture energy for all compositions was observed with annealing time as well as with annealing temperature.

It is well known that annealing changes the morphology in the photoactive layer [23]. Annealing the BHJ at temperatures higher than the glass transition temperature, which varies from 12.1 °C for pure P3HT to 131.2 °C for pure PCBM will make the polymers mobile [24]. As a consequence the P3HT forms ordered crystalline domains whereby the PCBM molecules diffuse outwards. Both the P3HT and PCBM domains grow laterally and an increase of vertical phase separation in BHJ takes place [23,25–28]. The lower surface energy polymer P3HT moves up towards the PEDOT:PSS interface, while the PCBM molecules tends to move towards the cathode side to form induced dipole–dipole bonds with ZnO layer. This is the driving force for vertical phase separation where a

Fig. 3. Fracture energy, G_c (J/m^2) as a function of the content of PCBM in the P3HT:PCBM layer showing a marked decrease with PCBM content. Silicon and polycarbonate were used as beam materials.
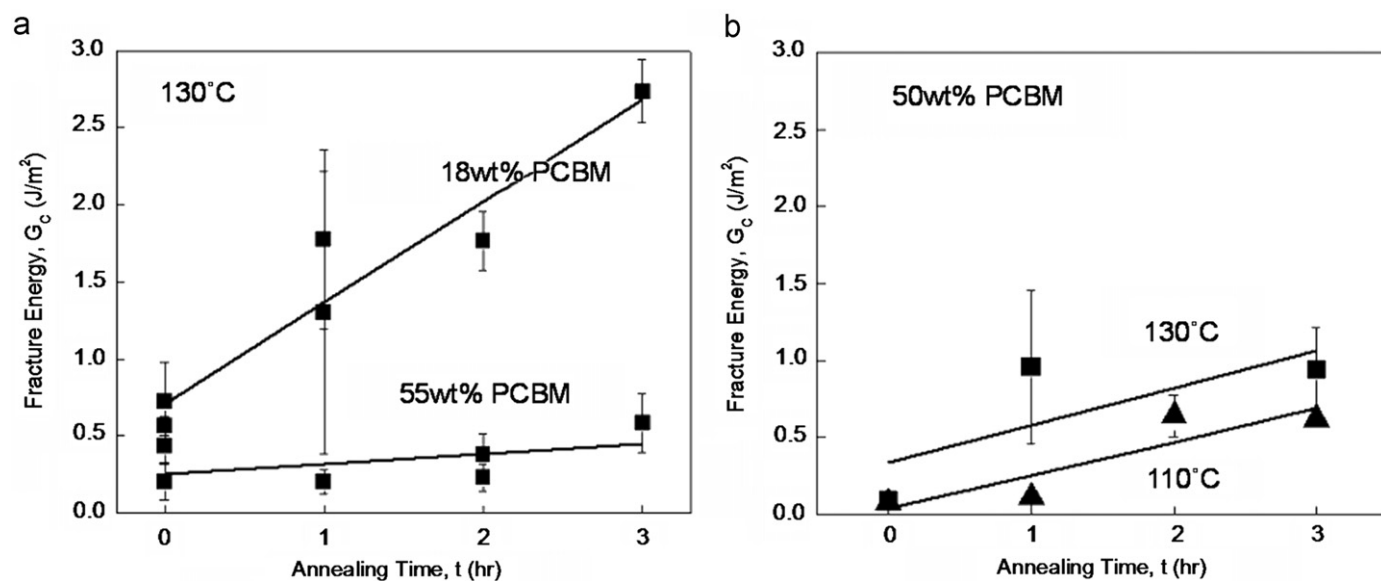

Fig. 4. Fracture energy, G_c (J/m^2) as a function of annealing time. (a) P3HT:PCBM solar cells with various weight percent ratios of PCBM in P3HT:PCBM annealed at 130 °C. (b) P3HT:PCBM solar cells with a 50 wt% PCBM annealed at 110 °C (triangle) and 130 °C (square).

higher concentration of P3HT develops at the PEDOT:PSS interface upon annealing.

These morphology changes alter the chemical properties at the interface. The increase of fracture energy can be partially explained by an increase of P3HT at the PEDOT:PSS interface, which is shown previously to form stronger bonds with PEDOT:PSS. It will be interesting in future studies to seek an optimal annealing time and temperature that benefit both adhesion and PCE. For example it was shown that larger crystals formed as a consequence of annealing enhance charge mobility, but once the domains are too large, short exciton lifetimes limit the exciton dissociation, resulting in loss of internal quantum efficiency.

3.3. HTL replacement

Since we observed weak adhesion between the BHJ and PEDOT:PSS HTL, delamination in PEDOT-free R2R inverted flexible polymer solar cells was studied. In this case the conductive polymer PEDOT:PSS was replaced with a metal oxide V_2O_5 HTL. The fracture energy, G_c for different film thicknesses of the V_2O_5 layer is shown in Fig. 5. The PCE for the R2R processed flexible V_2O_5 cells varied between 0.01% and 0.1% as previously reported [13]. Compared to the PEDOT:PSS cells, a two order of magnitude increase in G_c was observed at the expense of a marked decrease in PCE.

From XPS depth profiling we observed an intermixed layer between the V_2O_5 and the P3HT:PCBM layers of ~ 10 nm in thickness resulting in the strong interface between the HTL and BHJ. Adhesive failure between this intermixed layer and the BHJ was confirmed using XPS for all the HTL V_2O_5 layers.

The improved cohesion of the intermixed V_2O_5 and BHJ layer clearly evidences stronger molecular interactions. These may involve the formation of chemical bonds between molecules of the BHJ and V_2O_5 including possible covalent, ionic and bipolar interactions. In addition, the formation of the intermixed layer also involves an entangled molecular network and such molecular entanglements are well known to significantly increase fracture resistance in polymers [29–31]. Further elucidation of the contribution from such molecular interactions is the focus of ongoing studies. These effects, however, are clearly in stark contrast to the PEDOT:PSS layer that employs a fluorinated surfactant to enable wetting of the low surface energy P3HT:PCBM with the high surface tension PEDOS:PSS dispersion [32]. In addition, the fluorinated surfactants have earlier been shown to accumulate at the interface between the active layer and the PEDOT:PSS leading to weaker adhesion at the interface.

An increase in G_c with the thickness of the HTL V_2O_5 was observed and is shown in Fig. 5. Different thicknesses were produced by changing the concentration of VTIP in isopropanol (mg/ml), which was used to slot die coat the HTL on top of the P3HT:PCBM layer [13]. During drying the layer shrinks from 8 µm to hydrated vanadium oxide layer thicknesses in the range of 130 nm–185 nm thick depending on the initial concentration. There is a linear relation between the concentration of VTIP in isopropanol and the resulting thickness of the V_2O_5 layer. It is likely that the concentration of VTIP in the initial solution will have an impact on the interface properties, such as fracture energy and roughness, as well as on the morphology of the film itself. The increase of fracture energy with the thickness of V_2O_5 layer can be explained by a higher concentration of VTIP in the initial solution, resulting in stronger molecular interactions. However, the reason for the increased molecular interactions is currently unknown.

It should finally be stressed that for the thicknesses used in this study appreciable roughness will develop in the V_2O_5 layer. Previously, the formation of microscopic cracks was observed when V_2O_5 was employed as a recombination layer in tandem solar cells [33]. The roughness and interpenetration of the BHJ molecules into the cracked surface may contribute further to the increased adhesion observed for thicker V_2O_5 layers.

4. Conclusion

The interlayer adhesion in R2R processed flexible inverted P3HT:PCBM solar cells has been studied and quantified. Adhesive failure was observed between the bulk heterojunction P3HT:PCBM and adjacent conductive polymer layer PEDOT:PSS marked by low fracture energy values. The adhesion fracture energy varied from 1.6 J/m^2 to 0.1 J/m^2 depending on the composition of the P3HT:PCBM layer. Post deposition annealing time and temperature were shown to improve the adhesion at this interface. Additionally the PEDOT:PSS cells were compared with V_2O_5 cells whereby adhesive failure marked by high fracture energies was observed. Further studies will report on strategies to improve the adhesion at the respective interface HTL/BHJ by thermal and chemical treatments.

Acknowledgments

Fig. 5. Fracture Energy, G_c (J/m^2) as a function of the thickness of the HTL V_2O_5.

References

[1] C.J. Brabec, N.S. Sariciftci, J.C. Hummelen, Plastic solar cells, Advanced Functional Materials 11 (2001) 15–26.
[2] N.S. Sariciftci, L. Smilowitz, A.J. Heeger, F. Wudl, Photoinduced electron-transfer from a conducting polymer to buckminsterfullerene, Science 258 (1992) 1474–1476.
[3] F.C. Krebs, Fabrication and processing of polymer solar cells: a review of printing and coating techniques, Solar Energy Materials and Solar Cells 93 (2009) 394–412.
[4] B.C. Thompson, J.M.J. Frechet, Organic photovoltaics—polymer–fullerene composite solar cells, Angewandte Chemie International Edition 47 (2008) 58–77.
[5] G. Dennler, M.C. Scharber, C.J. Brabec, Polymer–Fullerene Bulk-Heterojunction Solar Cells, Advanced Materials 21 (2009) 1323–1338.
[6] F.C. Krebs, T. Tromholt, M. Jorgensen, Upscaling of polymer solar cell fabrication using full roll-to-roll processing, Nanoscale 2 (2010) 873–886.
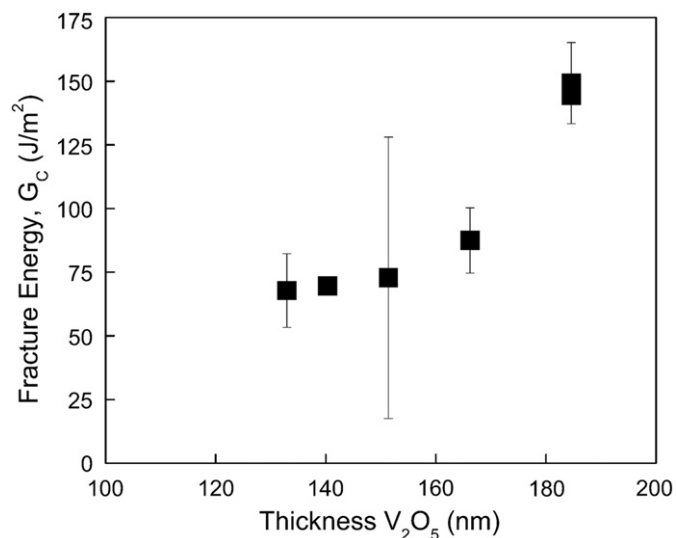
[7] V. Brand, C. Bruner, R.H. Dauskardt, Cohesion in organic bulk heterojunction solar cells, in preparation.

[8] L.F. Francis, A.V. McCormick, D.M. Vaessen, J.A. Payne, Development and measurement of stress in polymer coatings, Journal of Materials Science 37 (2002) 4717–4731.

[9] R. Dauskardt, M. Lane, Q. Ma, N. Krishna, Adhesion and debonding of multi-layer thin film structures, Engineering Fracture Mechanics 61 (1998) 141–162.

[10] J. Alstrup, M. Jorgensen, A.J. Medford, F.C. Krebs, Ultra fast and parsimonious materials screening for polymer solar cells using differentially pumped slot-die coating, ACS Applied Materials and Interfaces 2 (2010) 2819–2827.

[11] M. Jorgensen, K. Norrman, F.C. Krebs, Stability/degradation of polymer solar cells, Solar Energy Materials and Solar Cells 92 (2008) 686–714.

[12] F.C. Krebs, Degradation and stability of polymer and organic solar cells, Solar Energy Materials and Solar Cells 92 (2008) 685.

[13] N. Espinosa, H.F. Dam, D.M. Tanenbaum, J.W. Andreasen, M. Jorgensen, F.C. Krebs, Roll-to-roll processing of inverted polymer solar cells using hydrated vanadium (v) oxide as a pedot:pss replacement, Materials 4 (2011) 162–182.

[14] B.M. Sharratt, L.C. Wang, R.H. Dauskardt, Anomalous debonding behavior of a polymer/inorganic interface, Acta Materialia 55 (2007) 3601–3609.

[15] J.M. Snodgrass, D. Pantelidis, M.L. Jenkins, J.C. Bravman, R.H. Dauskardt, Subcritical debonding of polymer/silica interfaces under monotonic and cyclic loading, Acta Materialia 50 (2002) 2395–2411.

[16] M.S. Oliver, K.Y. Blohowiak, R.H. Dauskardt, Molecular structure and fracture properties of ZrOX/Epoxysilane hybrid films, Journal of Sol–Gel Science and Technology 55 (2010) 360–368.

[17] M.F. Kanninen, Augmented double cantilever beam model for studying crack-propagation and arrest, International Journal of Fracture 9 (1973) 83–92.

[18] J.Y. Oh, W.S. Jang, T.I. Lee, J.M. Myoung, H.K. Baik, Driving vertical phase separation in a bulk-heterojunction by inserting a poly(3-hexylthiophene) layer for highly efficient organic solar cells, Applied Physics Letters 98 (2011) 023303-1-023303-3.

[19] V. Brand, K. Levi, M.D. McGehee, R.H. Dauskardt, Film stresses and electrode buckling in organic solar cells, in preparation.

[20] A.R. Postema, A.T. Doornkamp, J.G. Meijer, H. Vandervlekkert, A.J. Pennings, Effect of chlorosulfonation of ultrahigh strength polyethylene fibers on mechanical-properties and bonding with gypsum plaster, Polymer Bulletin 16 (1986) 1–6.

[21] G. Fourche, An overview of the basic aspects of polymer adhesion part II: application to surface treatments, Polymer Engineering and Science 35 (1995) 968–975.

[22] S. Holmes, P. Schwartz, Amination of ultra-high strength polyethylene using ammonia plasma, Composites Science and Technology (1990) 1–21.

[23] X.N. Yang, J. Loos, S.C. Veenstra, W.J.H. Verhees, M.M. Wienk, J.M. Kroon, M.A.J. Michels, R.A.J. Janssen, Nanoscale morphology of high-performance polymer solar cells, Nano Letters 5 (2005) 579–583.

[24] J. Zhao, A. Swinnen, G. Van Assche, J. Manca, D. Vanderzande, B. Van Mele, Phase diagram of p3ht/pcbm blends and its implication for the stability of morphology, Journal of Physical Chemistry B 113 (2009) 1587–1591.

[25] S.S. van Bavel, M. Barenklau, G. de With, H. Hoppe, J. Loos, P3HT/PCBM bulk heterojunction solar cells: impact of blend composition and 3d morphology on device performance, Advanced Functional Materials 20 (2010) 1458–1463.

[26] M. Campoy-Quiles, T. Ferenczi, T. Agostinelli, P.G. Etchegoin, Y. Kim, T.D. Anthopoulos, P.N. Stavrinou, D.D.C. Bradley, J. Nelson, Morphology evolution via self-organization and lateral and vertical diffusion in polymer:fullerene solar cell blends, Nature Materials 7 (2008) 158–164.

[27] Y. Kim, S. Cook, S.M. Tuladhar, S.A. Choulis, J. Nelson, J.R. Durrant, D.D.C. Bradley, M. Giles, I. Mcculloch, C.S. Ha, M. Ree, A strong regioregularity effect in self-organizing conjugated polymer films and high-efficiency poly-thiophene:fullerene solar cells, Nature Materials 5 (2006) 197–203.

[28] Z. Xu, L.M. Chen, G.W. Yang, C.H. Huang, J.H. Hou, Y. Wu, G. Li, C.S. Hsu, Y. Yang, Vertical phase separation in poly(3-hexylthiophene):fullerene derivative blends and its advantage for inverted structure solar cells, Advanced Functional Materials 19 (2009) 1227–1234.

[29] R.H. Dauskardt, M.L. Jenkins, J.C. Bravman, Important factors for silane adhesion promoter efficacy: surface coverage, functionality and chain length, Journal of Adhesion Science and Technology 18 (2004) 1497–1516.

[30] D.B. Xu, C.Y. Hui, E.J. Kramer, C. Creton, A micromechanical model of crack-growth along polymer interfaces, Mechanics of Materials 11 (1991) 257–268.

[31] H.R. Brown, Adhesion between Polymers, IBM Journal of Research and Development 38 (1994) 379–389.

[32] F.C. Krebs, K. Norrman, M.V. Madsen, S.A. Gevorgyan, Degradation patterns in water and oxygen of an inverted polymer solar cell, Journal of the American Chemical Society 132 (2010) 16883–16892.

[33] T.T. Larsen-Olsen, T.R. Andersen, B. Andreasen, A.P.L. Bottiger, E. Bundgaard, K. Norrman, J.W. Andreasen, M. Jorgensen, F.C. Krebs, Roll-to-roll processed polymer tandem solar cells partially processed from water, Solar Energy Materials and Solar Cells (2011). doi:10.1016/j.solmat.2011.08.025.